Optimised strut and tie model for integrated ULS- and SLS design of RC structures

Larsen, J.; Poulsen, P. N.; Olesen, J. F.; Hoang, L. C.

Published in:
Computational Modelling of Concrete and Concrete Structures

Link to article, DOI:
10.1201/9781003316404-89

Publication date:
2022

Document Version
Publisher's PDF, also known as Version of record

Computational Modelling of Concrete and Concrete Structures – Meschke, Pichler & Rots (Eds)

Optimised strut and tie model for integrated ULS- and SLS design of RC structures

J. Larsen, P.N. Poulsen, J.F. Olesen & L.C. Hoang
Department of Civil Engineering, Technical University of Denmark, Kgs. Lyngby, Denmark

ABSTRACT: The structural designer has to take serviceability - and ultimate- limit states into account when choosing layout and materials as there exists no universally used tool, which can consider both simultaneously. A tool for the ultimate limit state is the Finite Element Limit Analysis, which can perform material optimisation on a ground structure, which has been proven effective. Here the serviceability limit state is adapted to fit the optimisation in order to handle both limit states simultaneously in a convex solver.

As a first step towards a general tool, the method is set up for bar elements and applied to concrete structures yielding a so-called strut and tie model. For simple ground structures, the tool reproduces known solutions. For large scale structures subjected to multiple load cases the tool shows good results but did suffer from minor numerical instabilities.

1 INTRODUCTION

When designing structures, the designer has to ensure that the structure adheres to requirements in both the Serviceability Limit State (SLS) and the Ultimate Limit State (ULS). Today many design tools exist that can help the designer. These tools can help by visualising the force distribution in the structure or help minimise the material usage through material optimisation. However, in general, these tools do not consider both SLS and ULS requirements simultaneously when doing the material optimisation. In ULS, very effective methods for solid concrete structures exist, which can find optimal designs of large scale structures with reasonable computational cost, e.g. Finite Element Limit Analysis (FELA) (Andersen, Poulsen, & Olesen 2022). These design tools utilise material optimisation on a ground structure as the method of finding optimised designs. The feasible set of FELA is convex, from which the global minimum is directly found by means of a convex solver.

For SLS structural optimisation, no universally used tool exists. One of the most commonly used elasticity based methods is Topology Optimisation (Bendsoe & Sigmund 2003). However, this method is based upon linear material models and is originally not suitable for modelling the non-linear behaviour of cracking in concrete. The cracking of concrete can be modelled with numerical tools, as seen in (Vestergaard, Larsen, Hoang, Poulsen, & Feddersen 2021), from which the current papers has drawn its inspiration. However, the referenced paper, does not performer material optimisation. In general, there is a lack of methods for material optimisation while considering the cracking of concrete. Thus a design tool taking into account the cracking of concrete, as well as both SLS and ULS requirements, is needed. The effectiveness of the methods for material optimisation in ULS applying FELA is due to the convex solver that effectively solves large-scale problems (Boyd & Vandenberghe 2004). To solve the combined problem of SLS and ULS requirements the aim is to also include the SLS requirements in the convex solver. However, the SLS requirements are non-convex.

For the convex solver to be used on a non-convex problem, the problem must be reformulated. Approximations can be made in several ways, such as linearisation of the model or second-order Taylor expansion. For the second order Taylor expansion, the hessian has to be positive-definite for a convex solver. If the hessian is not positive-definite, it can be approximated by removing the negative eigenvalues of the hessian (Duchi 2018). However, in this paper, only a first-order Taylor expansion is applied.

A first step in developing a general tool for solids is presented in this paper, where bar elements are used instead of solids. For reinforced concrete structures, the use of bar elements is often called a strut and tie model (Schlaich, Shafer, Jennewein, & Kotsovos 1987).

2 CONSTITUTIVE MODEL

To simulate the behaviour of reinforced concrete, a constitutive model is needed. The behaviour is approximated by a bi-linear model in both compression and tension, such that plastic and elastic behaviour can be represented. The difference in stiffness of concrete and reinforcement is furthermore included in the model.

DOI 10.1201/9781003316404-89

This leads to a quad-linear stress-strain curve which, as seen in Figure 1.

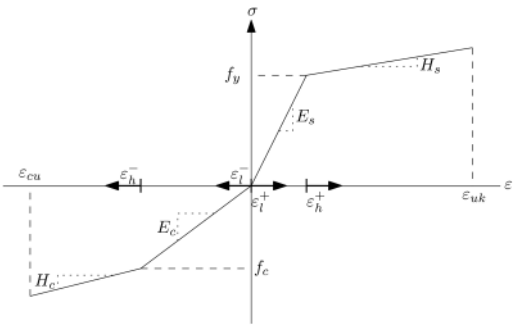

Figure 1. Constitutive model.

Where E_c and E_s are the young's moduli and H_c and H_s is the hardening modulus of concrete and reinforcement, respectively. f_c and f_s are the yield strengths, and ε_{cu} and ε_{uk} are the ultimate strain of concrete and reinforcement, respectively.

Table 1 shows the parameters used in the model. The values correspond to those found in (for Standardization 2005). The first set of parameters in Table 1 represents an SLS condition, i.e. a pure elastic behaviour, where no hardening is allowed, and the stresses are constrained to be within the pure elastic domain of reinforced concrete. The limit of the elastic regime is chosen to be half of the yield strength. The second set of parameters represents ULS conditions, where strains can reach the ultimate strain of the respective material.

Table 1. Material parameters.

SLS			
$\sigma_{c,max}$	$\varepsilon_{c,max}$	E_c	H_c
17.5 MPa	0.000515	34 GPa	6.63 Mpa
$\sigma_{s,max}$	$\varepsilon_{s,max}$	E_s	H_s
250 MPa	0.00125	200 Gpa	410 MPa
ULS			
f_c	ε_{cu}	E_c	H_c
35 MPa	0.0035	34 GPa	6.63 Mpa
f_y	ε_{uk}	E_s	H_s
500 MPa	0.05	200 Gpa	410 MPa

For modelling purposes, the strains in the model have to be split into different parts. The strains in an element are given as the sum of the concrete strains and the reinforcement strains. As the reinforcement is in tension it is given that $\varepsilon_l^- \geq 0$ and $\varepsilon_h^- \geq 0$. While for the concrete in compression, and the strains are thus negative, a minus is introduced such that $\varepsilon_l^+ \geq 0$ and $\varepsilon_h^+ \geq 0$. This is expressed as:

$$\varepsilon_e = \varepsilon_{l,e}^+ + \varepsilon_{h,e}^+ - \varepsilon_{l,e}^- - \varepsilon_{h,e}^-$$

This formulation does not ensure compatible solutions. However, as minimum potential energy is obtained, compatibility is ensured at the optimal point. To use this model in a FEM formulation the strains in the element, ε_e, is calculated as:

$$\varepsilon_e = \mathbf{B}_e \mathbf{v}_e \tag{1}$$

where $\mathbf{v}_e$ is the nodal displacement of element e and $\mathbf{B}_e$ is the global strain-displacement matrix as defined in e.g. (Kuna 2013).

3 MINIMUM POTENTIAL ENERGY

The principle of minimum potential energy is utilised to ensure an admissible displacement field, which states: The actual displacement, which satisfies stable equilibrium, renders the potential energy minimum.

The total potential energy can be found as the sum of the strain energy and the potential energy associated with applied forces:

$$E_{pot}^{tot} = E_{pot}^{in} + E_{pot}^{ext}$$

This method can find the displacement field for the quad-linear model without using a stiffness matrix.

The internal strain energy can be determined as the integration of the potential energy density.

$$E_{pot}^{in} = \int_\Omega P' \mathbf{d}\Omega$$

The strain energy is given as the absolute sum of areas under the stress-strain curve. This can be expressed through two triangular contributions from the concrete and reinforcement, along with a rectangular contribution from each material. This is expressed in Equation 2 for element e.

$$\begin{aligned}\int_{\Omega_e} P' \mathbf{d}\Omega_e = {} & \tfrac{1}{2} E_c A_{c,e} L_e (\varepsilon_{l,e}^-)^2 + \tfrac{1}{2} H_c A_{c,e} L_e (\varepsilon_{h,e}^-)^2 \\ & + \tfrac{1}{2} E_s A_{s,e} L_e (\varepsilon_{l,e}^+)^2 + \tfrac{1}{2} H_s A_{s,e} L_e (\varepsilon_{h,e}^+)^2 \\ & + A_{c,e} L_e f_c (\varepsilon_{h,e}^-) + A_{s,e} L_e f_y (\varepsilon_{h,e}^+)\end{aligned} \tag{2}$$

where $A_{s,e}$ and $A_{c,e}$ are the reinforcement and concrete areas of element e respectively, with L_e being the length of the element. P' is the potential energy density which is integrated over the domain Ω. This can be written as a second order equation:

$$\int_{\Omega_e} P' \mathbf{d}\Omega_e = \tfrac{1}{2} \mathbf{x}_e^{\mathrm{T}} \mathbf{Q}_e \mathbf{x}_e + \mathbf{c}_e^{\mathrm{T}} \mathbf{x} \tag{3}$$

Where $\mathbf{Q}_e$, $\mathbf{x}_e$ and $\mathbf{c}_e$ are given by

$$\mathbf{Q}_e = \begin{bmatrix} E_c A_{c,e} L_e & 0 & 0 & 0 \\ 0 & H_c A_{c,e} L_e & 0 & 0 \\ 0 & 0 & E_s A_{s,e} L_e & 0 \\ 0 & 0 & 0 & H_s A_{s,e} L_e \end{bmatrix}$$

$$\mathbf{x}_e = \begin{bmatrix} \varepsilon_{c,l,e} \\ \varepsilon_{c,h,e} \\ \varepsilon_{s,l,e} \\ \varepsilon_{s,h,e} \end{bmatrix}, \qquad \mathbf{c}_e = \begin{bmatrix} 0 \\ A_{c,e} L_e f_c \\ 0 \\ A_{s,e} L_e f_y \end{bmatrix}$$

The external potential energy can be found by the product of external forces and displacements, which can be expressed in a vectorised form, as seen below.

$$E_{pot}^{ext} = -\sum_i F_i u_i = -\mathbf{R}^{\mathrm{T}}\mathbf{V}$$

Where F is a force and u is the displacement. $\mathbf{R}$ is the nodal load vector, and $\mathbf{V}$ is the nodal displacement vector.

To find the displacement field that leads to minimum potential energy, a convex optimisation problem is presented. The objective is to minimise the potential energy while adhering to equilibrium and stress constraints, which is presented in Equation 4.

$$\text{Min.} \sum_{e=1}^{n_{el}} \gamma_e - \mathbf{R}^{\mathrm{T}}\mathbf{V} \tag{4a}$$

$$\text{S.t. } \mathbf{H}(\mathbf{E}\odot\mathbf{A}\odot\boldsymbol{\varepsilon}) = \mathbf{R} \tag{4b}$$

$$\mathbf{B}_e\mathbf{v}_e = \varepsilon_{l,e}^{+} + \varepsilon_{h,e}^{+} - \varepsilon_{l,e}^{-} - \varepsilon_{h,e}^{-}, \quad \forall e \tag{4c}$$

$$\tfrac{1}{2}\mathbf{x}_e^{\mathrm{T}}\mathbf{Q}_e\mathbf{x}_e + \mathbf{c}_e^{\mathrm{T}}\mathbf{x}_e - \gamma_e \le 0, \quad \forall e \tag{4d}$$

Where $\boldsymbol{\varepsilon}$ is a strain vector, and $\mathbf{H}$ is the equilibrium matrix (see e.g. (Damkilde 1991)), which is assembled from contributions of each element. $\mathbf{A}$ and $\mathbf{E}$ are the generalised areas and Young's moduli of the elements, consisting of contributions from the reinforcement and concrete for both $\mathbf{A}$ and $\mathbf{E}$, while contributions from both the linear and hardening stiffness are also given in $\mathbf{E}$. The symbol $\odot$ is the Hadamard product signifying entrywise product.

In Equation 4 the objective Equation 4a is to minimise the potential energy, Equation 4b is the equilibrium constraint, Equation 4c is the strain split constraint and Equation 4d is the constraint, defining the potential energy at the optimal point. It should be noted that equilibrium is ensured at the point of minimum potential energy. However, for the use with material optimisation, the equilibrium is also formulated explicitly.

This minimisation problem can be solved directly as the problem is convex, which it is since the objective along with the equilibrium, and yielding constraints are linear and thus convex. The potential energy constraint is, however quadratic, and is only convex if $\mathbf{Q}$ is symmetric and positive semidefinite, which is true as $\mathbf{Q}$ is diagonal with non-negative diagonal entries. This rotated quadratic cone can be assembled for all elements, such that a single cone can be used to represent the total potential energy of the structure. The inequality in Equation 4d is needed for convexity. However, in the case of minimum potential energy, the inequality becomes an equality.

4 MATERIAL OPTIMISATION

The theory of minimum potential energy will lead to a stable deformation field and thus an admissible strut and tie model. However, this is not a optimal model as redundant material might be used. Thus the use of material optimisation is needed. The areas of reinforcement and concrete are introduced as variables. This is added as an objective function, along with the potential energy, which leads to the following multi-criterion optimisation problem.

$$\begin{aligned}
&\text{Min.} \left[\textstyle\sum_{e=1}^{n_{el}} \gamma_e - \mathbf{R}^{\mathrm{T}}\mathbf{V} \ \sum_{e=1}^{n_{el}} \left(\frac{f_y}{f_c}A_{s,e} + A_{c,e}\right)\right]^{\mathrm{T}} \\
&\text{S.t. } \mathbf{H}(\mathbf{E}\odot\mathbf{A}\odot\boldsymbol{\varepsilon}) = \mathbf{R} \\
&\qquad \mathbf{B}_e\mathbf{v}_e = \varepsilon_{l,e}^{+} + \varepsilon_{h,e}^{+} - \varepsilon_{l,e}^{-} - \varepsilon_{h,e}^{-}, \quad \forall e \\
&\qquad \int_{\Omega_i} P' \mathrm{d}\Omega_e \le \gamma_e, \quad \forall e
\end{aligned}$$

The problem is, however, non-convex, which can be seen by investigating the potential energy density given by the first equation in Equation 2. It is noted that this is given as a third-order polynomial, which can never be convex. To solve the problem, a sequential convex program is formulated, where a series of convex approximations of the problem is solved.

4.1 *Local convex approximation*

The potential energy density defined by Equation 2, where the reinforcement and concrete areas and strains are split into an increment and a value given from the former iteration. This is illustrated for the reinforcement area in Equation 5.

$$A_{s,e} = A_{s,0,e} + \Delta A_{s,e} \tag{5}$$

The same is introduced for the concrete area, as well as all strains. When introduced into Equation 2 a third order equation arises, which is approximated by a first-order Taylor expansion, leading to a purely linear model, as seen in Equation 6.

$$\begin{aligned}
&\int_{\Omega_e} P' \mathbf{d}\Omega_e \approx \mathbf{c}_{lin,e}^{\mathrm{T}}\Delta\mathbf{x}_e, \quad \Delta\mathbf{x}_e = \begin{bmatrix} \Delta\varepsilon_{l,e}^{-} \\ \Delta\varepsilon_{h,e}^{-} \\ \Delta\varepsilon_{l,e}^{+} \\ \Delta\varepsilon_{h,e}^{+} \\ \Delta A_c \\ \Delta A_s \end{bmatrix} \\
&\mathbf{c}_{lin,e} = \begin{bmatrix} L_e E_c A_{c,0,e}\varepsilon_{l,0,e}^{-} \\ L_e H_c A_{c,0,e}\varepsilon_{h,0,e}^{-} + L_e f_{ck} H_c \varepsilon_{h,0,e}^{-} \\ L_e E_s A_{s,0,e}\varepsilon_{l,0,e}^{+} \\ L_e H_s A_{s,0,e}\varepsilon_{h,0,e}^{+} + L_e f_y L H_s \varepsilon_{h,0,e}^{+} \\ \frac{L_e}{2}\left(E_c(\varepsilon_{l,0,e}^{-})^2 + H_c(\varepsilon_{h,0,e}^{-})^2\right) + f_{ck}\varepsilon_{h,0,e}^{-} \\ \frac{L_e}{2}\left(E_s(\varepsilon_{l,0,e}^{+})^2 + H_s(\varepsilon_{h,0,e}^{+})^2\right) + f_y\varepsilon_{h,0,e}^{+} \end{bmatrix}
\end{aligned} \tag{6}$$

This can be formulated as an equality constraint, as it is linear and convex.

The equilibrium constraint can be proven to be non-convex, by writing it in a second order form, and proving that the matrix coefficient of the second order term is not positive-semidefinite. Thus a approximation based upon a first order Taylor expansion is used:

$$\mathbf{H}(\mathbf{E}\odot\mathbf{A}_0\odot\Delta\boldsymbol{\varepsilon} + \mathbf{E}\odot\Delta\mathbf{A}\odot\boldsymbol{\varepsilon}_0) \approx \mathbf{R} - \mathbf{H}_0 \tag{7}$$

where $\mathbf{H}_0 = \mathbf{H}(\mathbf{E} \odot \mathbf{A}_0 \odot \boldsymbol{\varepsilon}_0)$. This approximation is obviously linear and thus convex. The yielding constraints are still found to be linear and are thus convex as is.

The convex approximations are only viable when the changes are small. A limit on the design variables is thus implemented, through a box constraint, to ensure adequately good approximations. These approximations also turn the second-order cone program described in Equation 4 into a linear program.

4.2 Weighted sum method

The weighted sum method is used to solve the multi-criterion optimisation problem, where the two objectives are combined in a weighting sum. If the weighting on the potential energy is high, the algorithm will increase the material to minimise the potential energy. If the weight is low, minimum potential energy will not be guaranteed for the observed structure. The weighting is chosen as unity on the material optimisation and a weighting of α_{ws} on the potential energy. This leads to the following problem.

$$\begin{aligned} \text{Min. } & \alpha_{ws} \left(\sum_{e=1}^{n_{el}+1} \gamma_e - \mathbf{R}^{\mathrm{T}} \mathbf{V} \right) + \sum_{e=1}^{n_{el}} \frac{f_y}{f_c} A_{s,e} + A_{c,e} \\ \text{S.t. } & \mathbf{H}(\mathbf{E} \odot \mathbf{A}_0 \odot \Delta\boldsymbol{\varepsilon} + \mathbf{E} \odot \Delta\mathbf{A} \odot \boldsymbol{\varepsilon}_0) = \mathbf{R} - \mathbf{H}_0 \\ & \mathbf{B}_e \mathbf{v}_e = \varepsilon^+_{l,e} + \varepsilon^+_{h,e} - \varepsilon^-_{l,e} - \varepsilon^-_{h,e}, \quad \forall e \\ & \mathbf{c}_{lin,e} \mathbf{x}_{lin,e} = \gamma_e, \quad \forall e \end{aligned} \tag{8}$$

With the volume given in m^3 and the potential energy given in MJ, it was empirically found that a weighting of $\alpha_{ws} = 10^{-2}$ lead to reliable results.

A pseudo-code that represents the algorithm can be seen in Algorithm 1.

Algorithm 1: Pseudo-code for the sequential convex program for strut and tie.

```
Initialisation of Topology;
FELA;
Update Areas;
Solve Equation 4;
Define Strains;
for i = 1 To n do
    Solve Equation 8;
    Update Areas;
    Solve Equation 4;
    Define Strains;
end
```

Note that Equation 8 utilise changes of design variables and is solved through approximations, while Equation 4 is solved with the total design variables and is solved precisely in each iteration.

4.3 Multiple load cases for different limit states

The method is expanded to contain several load cases where each load case can be of a different limit state. This is done by allocating the respective material properties to each load case, depending on if the calculations belong to SLS or ULS. Each new load case will introduce new strain variables, each independent of the other load cases. However, the cross-sectional areas are shared between all load cases.

5 RESULTS

The method will be applied to two examples, where the solution is presented.

5.1 Example 1 – deep beam

The first example is a deep beam loaded at the quarter-point. The structure is illustrated in Figure 2.

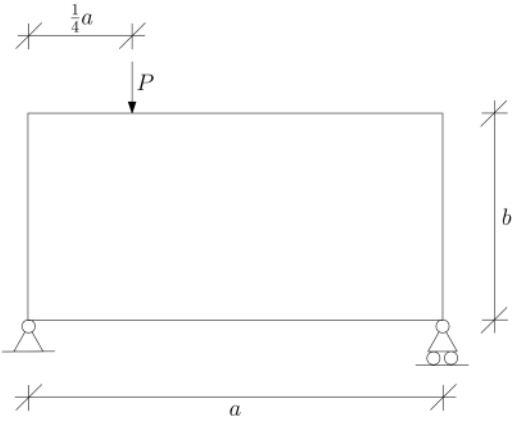

Figure 2. First Example - deep beam.

The example will be investigated for two different ground structures. The first one is given as coarse mesh, while the second will be for a finer mesh. The parameters for the model are summarised in Table 2.

Table 2. Parameters for example 1.

a	b	P	Limit State
5 m	10 m	200 kN	ULS

First, the coarse ground structure is chosen, with 15 nodes, where each node is connected to other nodes by bar elements, leading to a total of 105 elements. The ground structure, as well as the optimised structure, can be seen in Figure 3 and Figure 4 respectively.

The optimised strut and tie is seen to be relatively simple and is verifiable by hand calculation.

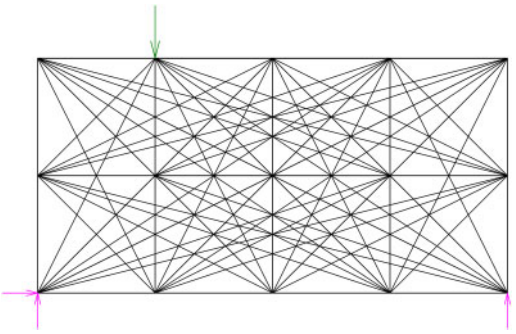

Figure 3. Course ground structure of first example.

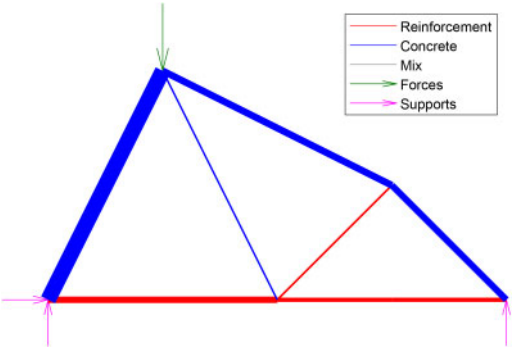

Figure 4. Optimised structure of first example with course ground structure. Only elements with a capacity of more than 1% of the highest capacity is plotted.

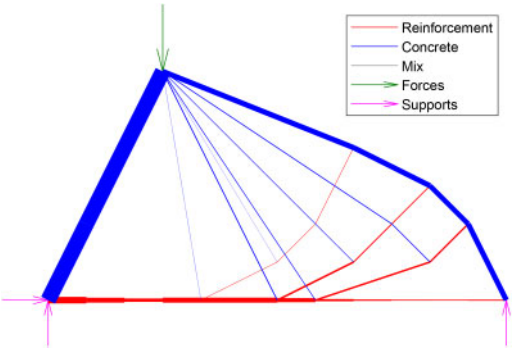

Figure 5. Optimised structure of first example with fine ground structure. Only elements with a capacity of more than 1% of the highest capacity is plotted.

As stated, the example is also investigated with a much finer mesh, given by 153 nodes, which are connected with elements, leading to 11628 elements.

The results in Figure 5 is seen to be similar to a well-known Michell structure (Michell 1904). Notably, some bars seem to change thickness, even though there is no joint with other elements. This is due to the number of elements connecting to each node along with the elements. These elements are tiny in area and are thus below the plotting threshold. However, the sum of the normal forces in these elements is enough to accumulate a significant force to facilitate these changes in thickness.

An example is also run to investigate if the Michell structure is also present for two load cases, where a second load case is added, with an equal force in the 3/4 point.

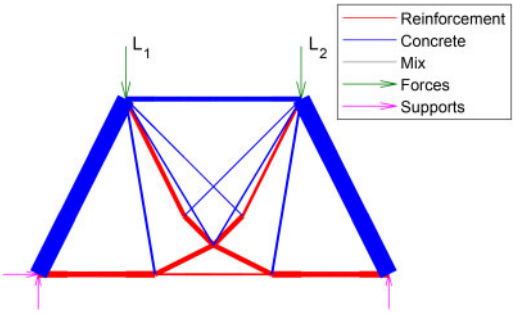

Figure 6. First example with fine ground structure and two load cases. Only elements with a capacity of more than 1% of the highest capacity is plotted. L_1 and L_2 indicates the loads for the first and second load case respectively.

Here the Michell-like structure disappears, and a more straightforward structure is achieved.

To investigate the robustness of the solution, the coarse mesh is also optimised based upon a homogeneous initial guess of material instead of a FELA optimised initial guess. When doing this, the solutions converged slowly to the same solution as the initial guess of FELA, indicating that even though the method is non-convex and globally optimal solutions are not guaranteed, the method seems to find solution solutions close to the initial guess of FELA.

5.2 Example 2 – multi-storey shear wall

The second example is given as a multi-storey shear wall with holes, which can be seen in Figure 7.

Each floor of the wall is 5 m wide and 5 m tall. Furthermore, the door opening is 1 m wide and 3 m tall. The structure is loaded by four different load cases, which are summarised in Table 3.

The ground structure, along with the optimised strut and tie, can be seen in Figure 8 and Figure 9 respectively.

It is noted that the optimised strut and tie is too complex to be found by hand and probably also too complex ever to be built in reality. However, this model could be used for an engineer to understand the stress distribution and create a simpler strut and tie model based upon the material distribution.

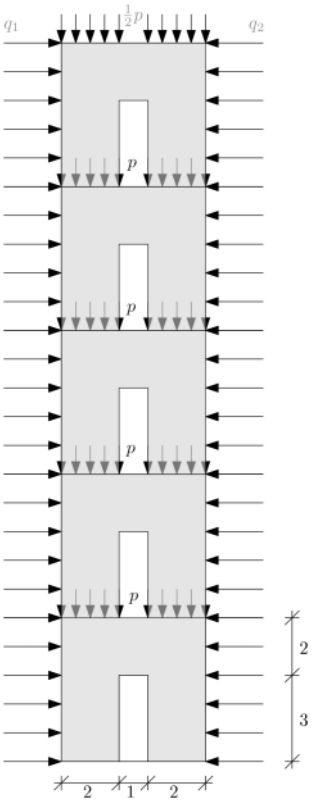

Figure 7. Mesh of structure for second example.

Table 3. Load cases for example 2.

Load Case	q_1 kN/m	q_2 kN/m	p kN/m	Limit state
1	20	0	30	ULS
2	0	20	30	ULS
3	13.3	0	30	SLS
4	0	13.3	30	SLS

6 DISCUSSION

The strut and tie models found by the method are seen to be very complex, and some post-processing is needed. The strut and tie models often produce Michell-like structures and would thus lead to designs where reinforcement bars need to be bent into curves, which is often not practical. Thus the designs should be used as an initial model for understanding the stress-distribution in the structure, and a simpler and reasonable strut and tie model could be created based upon the knowledge acquired. Furthermore, the local stress state in the nodes have to be investigated, however this is not considered in this paper.

When investigating example 2, the method was unstable, and the optimisation could become infeasible before convergence. This behaviour was especially

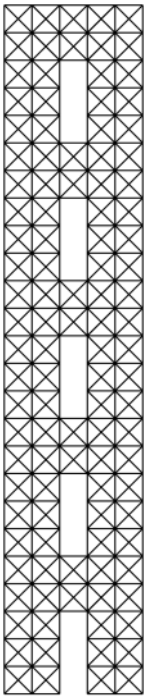

Figure 8. Ground structure of second example.

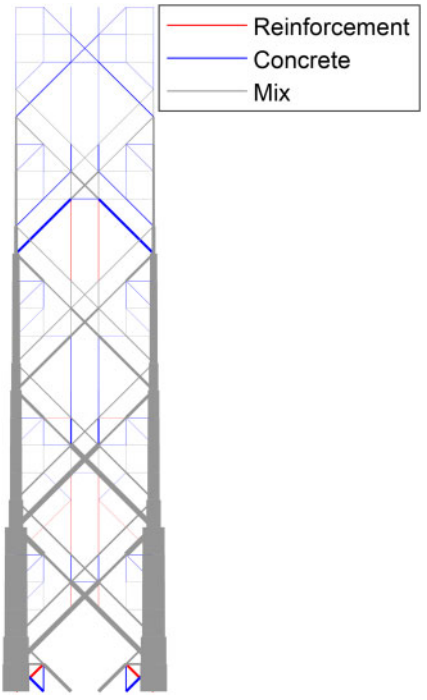

Figure 9. Optimised structure of Second example with course ground structure. Only elements with a capacity of more than 1% of the highest capacity is plotted.

present when optimising for many load cases simultaneously. This is a problem that can occur when performing sequential convex programming (Duchi 2018).

This is thought to be caused by the narrow solution space of the elastic solutions. Widening of the solution space might lead to better stability, which could be done through relaxation of the constraints. To ensure that the method will converge to a feasible solution, when the relaxation is applied, a penalty function could be introduced, where the constraints are introduced into the objective function, such that relaxation of the constraints are allowed at a price.

Along with this an obvious next step is to expand the method to 3-dimensional solid elements, such that realistic structures can be represented.

7 CONCLUSION

In this paper, a method for finding Strut and Tie models for reinforced concrete structures, subjected to both SLS and ULS load cases is presented.

The method suffers from instability and effectiveness issues, which was mostly seen for large scale structures, especially when subjected to many load cases, where the sequential convex programming could be infeasible after some iterations, before convergence was achieved. The convergence of the methods is also quite slow as the step-size has to be small to mitigate this instability. However, for simple structures, well-known solutions were reproduced, with Michell-like structures being achieved for fine meshed ground structures. The method also produced reliable results for relative complex structures, which were loaded with multiple load cases where both SLS and ULS were considered, despite the instability and effectiveness issues stated earlier.

REFERENCES

Andersen, M., P. N. Poulsen, & J. F. Olesen (2022). Partially mixed lower bound constant stress tetrahedral element for finite element limit analysis. *Computers & Structures 258*.

Bendsoe, M. & O. Sigmund (2003). *Topology Optimization: Theory, Methods, and Applications*. Springer Berlin Heidelberg.

Boyd, S. & L. Vandenberghe (2004). *Convex Optimization*. Cambridge University Press.

Damkilde, L. (1991). An efficient implementation of limit state calculations based on lower-bound solutions. In *Proceedings of Fourth Nordic Seminar on Computational Mechanics*.

Duchi, J. (2018). *Sequential Convex Programming*. Stanford Universit.

for Standardization, E. C. (2005). *EN 1992-1-1 Eurocode 2: Design of concrete structures - Part 1-1: General ruels and rules for buildings*. CEN.

Kuna, M. (2013, 01). *Finite elements in fracture mechanics: Theory – Numerics – Applications*, Volume 201. Springer Berlin Heidelberg.

Michell, A. (1904). The limits of economy of material in frame-structures. *The London, Edinburgh, and Dublin Philosophical Magazine and Journal of Science 8*(47), 589–597.

Schlaich, J., K. Shafer, M. Jennewein, & M. Kotsovos (1987, 05). Toward a consistent design of structural concrete. *PCI Journal 32*, 74–150.

Vestergaard, D., K. Larsen, L. Hoang, P. Poulsen, & B. Feddersen (2021). Design-oriented elasto-plastic analysis of reinforced concrete structures with in-plane forces applying convex optimization. *Structural Concrete 22*(6), 3272–3287.